$La_{1-x}Sr_xMnO_3$ ($x = 0, 0.3, 0.5, 0.7$) Nanoparticles Nearly Freestanding in Water: Preparation and Magnetic Properties

Yang Tian, Dairong Chen,* and Xiuling Jiao*

Department of Chemistry, Shandong University, Jinan 250100, P. R. China

Received September 18, 2006
Revised Manuscript Received November 13, 2006

The $La_{1-x}Sr_xMnO_3$ (LSMO) materials exhibit extensive potential applications in many fields such as data storage, solid oxide fuel cell (SOFC), pollution control for automotive exhausts, etc., because of their remarkable properties.[1] Devices for these applications are often fabricated using particulate-based methods including screen-printing, slurry or spin-coating, colloidal spray deposition and tape-casting, followed by a ceramic sintering process.[2] For these processes, nanoparticles free of agglomerates (micrometer-sized), especially those dispersed in water, are ideal.[3] Recently, some single metal oxide nanoparticles without agglomeration in water were prepared by various processes,[4] but those synthetic strategies are limited in the preparation of bi- or multi-metal oxides because of their complexity, including accurate stoichiometry, highly mixable precursors, specific chemistry for each phase, and high temperature of crystallization.[5] For the preparation of LSMO particles, although many methods, including sol−gel, coprecipitation, spray pyrolysis, combustion synthesis, and hydrothermal reaction, have been developed,[6] the routes to agglomerate-free, homogeneous LSMO nanoparticles have never been reported.

In this communication, a facile molten salt synthetic route, which was followed by dissolving the salts with the 2-pyrrolidone, to aggregate-free LSMO nanoparticles dispersed in water is introduced. Furthermore, the magnetic properties of LSMO nanoparticles are measured, and the interesting finding is that the LSMO nanoparticles exhibit exchange bias (EB), a shift in the hysteresis loop of ferromagnet. The EB phenomenon is usually found in bi- or multilayer films[7] and core−shell systems[8] but in few crystalline nanoparticles of magnetic materials.[9]

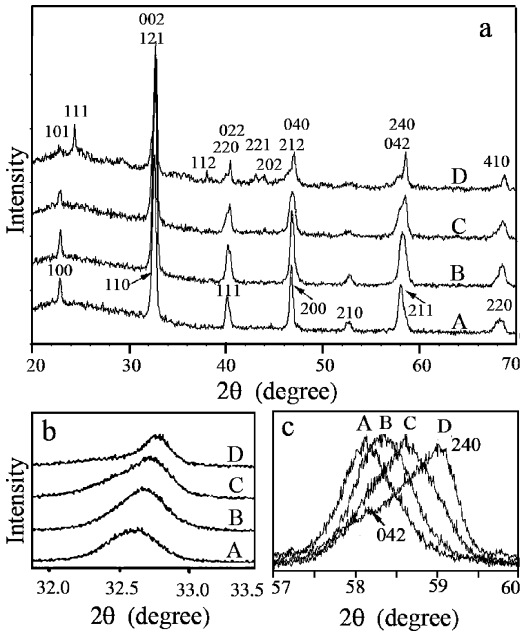

Figure 1. XRD patterns of (a) the prepared LSMO nanoparticles and of elaborate scan for samples around (b) 32.5 and (c) 58°. $x = 0$, 0.3, 0.5, 0.7 are represented as A, B, C, and D, respectively, in images.

To prepare LSMO nanoparticles, we used the molten $NaNO_3$ and KNO_3 mixture as solvent and applied the nitrates of La, Mn, and Sr as reagents. The resulting molten solid was placed in hot 2-pyrrolidone; the precipitate was separated by centrifugation and washed with ethanol. The crystalline LSMO with different x usually exhibit different structures because of their sensitivity to the internal pressure, which changes both the Mn−O bond distances and Mn−O−Mn bond angles.[10] The XRD patterns (Figure 1a) for the samples indicate the formation of a highly crystalline perovskite phase. All peaks for $x = 0$ can be indexed to the cubic phase, and the calculated lattice constant is $a = 3.876$ Å, which is in good agreement with the literature result of 3.880 Å (JCPD 75-0440). With the increasing content of doped Sr, the peaks appear to right shift (Figure 1b), indicating the contraction of the crystal cell, which is due to the changed oxidation state of Mn. However, for the Sr doping samples, the (211) peak gradually splits into (042) and (240) peaks (Figure 1c), illustrating the structural transition from cubic to ortho-

* Corresponding author. E-mail: cdr@sdu.edu.cn. Tel: 86-0531-88364280.

(1) (a) Levy, P. M. *Science* **1992**, *256*, 972. (b) Pena, M. A.; Fierro, J. L. G. *Chem. Rev.* **2001**, *101*, 1981. (c) Park, J.-H.; Vesocovo, E.; Kim, H.-J.; Kwon, C.; Ramesh, R.; Venkatesan, T. *Nature* **1998**, *392*, 794.
(2) Chervin, C. N.; Clapsaddle, B. J.; Chiu, H. W.; Gash, A. E.; Satcher, J. H., Jr.; Kauzlarich, S. M. *Chem. Mater.* **2006**, *18*, 1928.
(3) (a) Houivet, D.; El Fallah, J.; Haussonne, J.-M. *J. Am. Ceram. Soc.* **2002**, *85*, 321. (b) Petruska, M. A.; Malko, A. V.; Voyles, P. M.; Klimov, V. I. *Adv. Mater.* **2003**, *15*, 610.
(4) (a) Frankamp, B. L.; Fischer, N. O.; Hong, R.; Srivastava, S.; Rotello, V. M. *Chem. Mater.* **2006**, *18*, 956. (b) Wang, Y.; Wong, J. F.; Teng, X.; Lin, X. Z.; Yang, H. *Nano Lett.* **2003**, *3*, 1555. (c) Kim, M.; Chen, Y.; Liu, Y.; Peng, X. *Adv. Mater.* **2005**, *17*, 1429. (d) Fan, H.; Leve, E.; Gabaldon, J.; Wright, A.; Haddad, R. E.; Brinker, C. J. *Adv. Mater.* **2005**, *17*, 2587. (e) Li, Z.; Chen, H.; Bao, H.; Gao, M. *Chem. Mater.* **2004**, *16*, 1391. (f) Li, Z.; Sun, Q.; Gao, M. *Angew. Chem., Int. Ed.* **2005**, *44*, 123.
(5) David, G.; Cédric, B.; Berand, S.; Torsten, B.; Nicola, P.; Pierre, A. A.; Heinz, A.; Markus, A.; Clément, S. *Nat. Mater.* **2004**, *3*, 787.
(6) (a) Spooren, J.; Rumplecker, A.; Millange, F.; Walton, R. I. *Chem. Mater.* **2003**, *15*, 1401. (b) Urban, J. J.; Ouyang, L.; Jo, M.-H.; Wang, D. S.; Park, H. *Nano Lett.* **2004**, *4*, 1547. (c) Shen, S.-T.; Weng, H.-S. *Ind. Eng. Chem. Res.* **1998**, *37*, 2654. (d) Song, K. S.; Cui, H. X.; Kim, S. D.; Kang, S. K. *Catal. Today* **1999**, *47*, 155. (e) Aruna, S. T.; Muthuraman, M.; Patil, K. C. *J. Mater. Chem.* **1997**, *7*, 2499.
(7) (a) Ke, X.; Rzchowski, M. S. *Appl. Phys. Lett.* **2004**, *84*, 5458. (b) Panagiotopoulos, I.; Christides, C.; Moutis, N.; Niarchos, D. *J. Appl. Phys.* **1999**, *85*, 4913.
(8) (a) Masals, O.; Seshadri, R. *J. Am. Chem. Soc.* **2005**, *127*, 9354. (b) Si, P. Z.; Li, D.; Lee, J. W.; Choi, C. J.; Zhang, Z. D.; Geng, D. Y. *Appl. Phys. Lett.* **2005**, *87*, 133122.
(9) (a) Mishra, S. R.; Losby, J.; Dubenko, I.; Roy, S.; Ali, N.; Marasinghe, K. *J. Magn. Magn. Mater.* **2004**, *279*, 111. (b) Punnoose, A.; Seehra, M. S. *J. Appl. Phys.* **2002**, *91*, 7766.
(10) (a) Hemberger, J.; Krimmel, A.; Kurz, T.; Krug Von Nidda, H.-A.; Ivanov, V. Y.; Mukhin, A. A.; Balbashov, A. M.; Loidl, A. *Phys. Rev. B* **2002**, *66*, 94410. (b) Bindu, R. *Eur. Phys. J. B* **2004**, *37*, 321.

10.1021/cm0622349 CCC: $33.50
Published on Web 11/29/2006

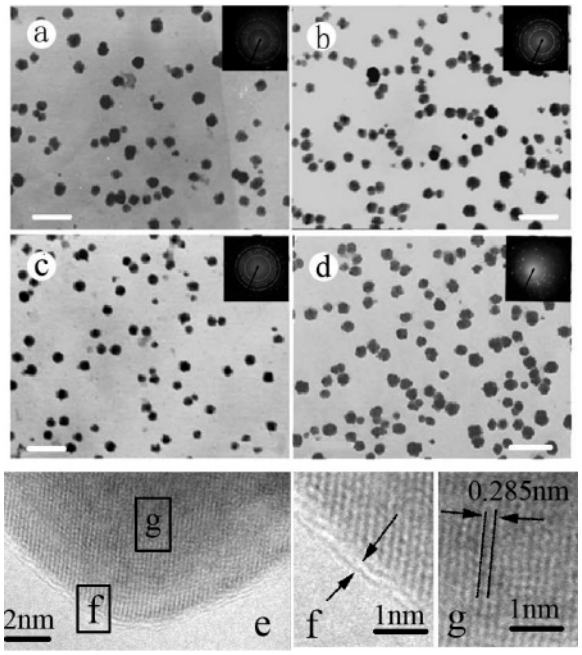

Figure 2. TEM ((a) $x = 0$, (b) $x = 0.3$, (c) $x = 0.5$, (d) $x = 0.7$) and HR-TEM ((e, f) $x = 0$) images of LSMO samples. The scale bars in Figure 2a−d are 100 nm, and the insets in Figure 2a−d are the corresponding SAED patterns.

rhombic (space group *Pbnm*) structure, which is different from those of the corresponding bulk materials. The LSMO bulks usually exhibit as hexagonal ($0.1 < x < 0.4$) and orthorhombic ($0.5 < x < 0.8$) phases;[10b] this difference might be due to the small size of LSMO nanoparticles and a large surface strain affecting the crystal lattice distortion. In addition, a small peak at ca. 29° appears in the XRD pattern of the sample for $x = 0.7$, indicating the formation of a small amount of La_2O_3 impurity (JCPDS 83-1350), which is due to the higher nucleation energy barrier for LSMO crystals with the increasing Sr content. Furthermore, the average sizes of the samples for $x = 0$, 0.3, 0.5, and 0.7 are calculated to be 19.5, 20.0, 19.0, and 25.3 nm, respectively, using the Scherrer formula according to the full width at half-maximum (fwhm) of (110) ($x = 0$) or (121) ($x > 0$) reflections.

The representative TEM images (Figure 2) reveal that the LSMO particles have a size of ca. 20 ± 5 nm, which is roughly close to the calculated results from the XRD patterns. All the samples appear to be almost-aggregate-free spherical particles in water. The SAED patterns (the insets in Figure 2a−d) confirm their crystalline nature, but the HR-TEM images (Figure 2e,f) show an organic layer coating on the nanoparticle's surface. The lattice spacing accorded with the {110} plane of cubic $LaMnO_3$ is ca. 2.85 Å (Figure 2g). The EDX analyses (see the Supporting Information) indicate that all samples are consistent with their element signals and stoichiometry as expected within the error. The LSMO nanoparticles are dispersed in water to form a clear solution and do not deposit even after standing for several weeks, exhibiting a good dispersibility (see the Supporting Information).

The organic compounds on the as-prepared LSMO nanoparticle's surface were studied by the thermal gravimetric (TG) and FT−IR analyses. The TG curve of $LaMnO_3$ nanoparticles (see the Supporting Information) indicates a

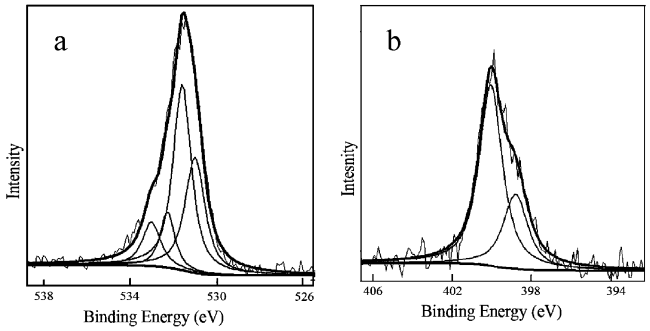

Figure 3. XPS spectra of the as-prepared $LaMnO_3$ nanoparticles for (a) O 1s and (b) N 1s.

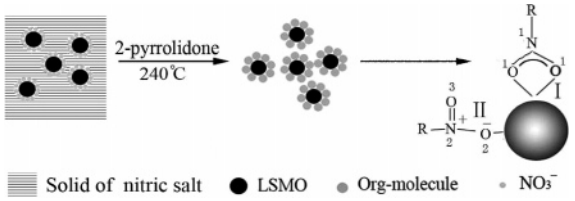

Figure 4. The dsorption of organic molecules on the nanoparticles

weight loss of ca. 16.9%, which hardly changes with the doped Sr content. The IR spectrum of $LaMnO_3$ (see the Supporting Information) shows two peaks at 1559 and 1408 cm^{-1}, corresponding to the stretching vibrations of N═O and C−N═O bonds of the NO_2 group. A weak absorption centered at 2900 cm^{-1} is assigned to C−H stretching vibrations, and the sharp peak at 1461 cm^{-1} is brought by the bending vibrations of C−H. However, both the ν_{N-H} band at 3241 cm^{-1} and the $\nu_{C=O}$ band at 1690 cm^{-1} that are attributed to 2-pyrrolidone vanish. Thus, the organic composition on the LSMO particles is the nitryl compound ($C_3H_7NO_3$), indicating that 2-pyrrolidone decomposes during the refluxing process.

The coordination of organic compounds with the nanoparticles can be proved by XPS character (Figure 3) for elements N and O, as shown in Figure 4. As is well-known, the binding energy will shift to lower values as N or O atoms bind to metals because of a transfer of electron density from N or O to metals.[11] Figure 3a shows the peak features related to four distinct environments of O atoms. The peak at 530.9 eV is the O1s of inorganic compound,[12] that at 531.6 eV is the O1s coordinated to the metals with two O atoms in the nitryl together (shown as O1 in Figure 4), the peak at 532.3 eV is the O1s that one O atom in the nitryl coordinates to the metals alone (shown as O2 in Figure 4), the peak at 533.0 eV is the O1s that one O atom in the nitryl does not coordinate to the metals (shown as O3 in Figure 4).[13] Furthermore, Figure 3a shows that the peak area of the O2 atom is nearly same as that of O3, which illustrates that their molar ratio is 1:1. It is calculated that the molar ratio of two coordinated molecules I and II is ca. 2.2. However, the

(11) (a) Wu, J. B.; Lin, Y. F.; Wang, J.; Chang, P. J.; Tasi, C. P.; Lu, C. C.; Yang, Y. W. *Inorg. Chem.* **2003**, *42*, 4516. (b) Charlier, J.; Cousty, J.; Xie, Z. X.; Poulennec, V. L.; Bureau, C. *Surf. Interface Anal.* **2000**, *30*, 283.
(12) Dzhurinskii, B. F.; Gati, D.; Sergushin, N. P.; Nefedov, V. I.; Salyn, Y. V. *Russian J. Inorg. Chem.* **1975**, *20*, 2307.
(13) Kakar, S.; Nelson, A. J.; Treusch, R.; Heske, C.; Van Buuren, T.; Jimenez, I.; Pagoria, P.; Terminello, L. J. *Phys. Rev. B* **2000**, *62*, 15666.

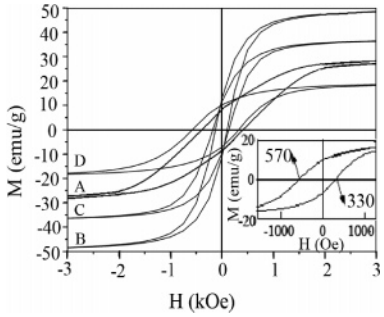

Figure 5. Magnetization as a function of the applied magnetic field for all samples at 5 K between +3 kOe and −3 kOe. $x = 0$, 0.3, 0.5, 0.7 are represented as A, B, C, and D, respectively. The inset is the enlarged magnetization curve of $La_{0.3}Sr_{0.7}MnO_3$.

number of O atoms in the inorganic compound is less than that in organic compound because the XPS detects only inorganic compounds on the surface of nanoparticles and not all of the the inorganic compound. On the other hand, Figure 3b shows the peak features related to two distinct environments of N atoms. The peaks at 399.8 and 398.8 eV correspond to the N1 and N2 of the nitryl, respectively, in Figure 4,[13] and their molar ratio (equal to the ratio of molecules I and II) is about 2.3:1 calculated from the peak areas, similar to the above result. The results are different from those in Gao's report, who reported the organic composition was amine.[4e,f] This difference might be caused by the different reaction conditions; in the present work, the atmosphere was air, and that in Gao's work was N_2 flow. Thus, the XPS analysis indicates that the nitryl compound is coordinated to the nanoparticles by O atoms to form a stable organic shell and prevents them from aggregating. After the LSMO nanoparticles formed in molten salt are dissolved in 2-pyrrolidone, the organic solvents gradually decompose to form the nitryl compound, which replaces the anions such as NO_3^- adsorbed on the nanoparticle's surface. The nitryl compound might be coordinated to the nanoparticle by two styles (shown as I and II in Figure 4).

The magnetic properties of the as-prepared nanoparticles were investigated with a Quantum magnetometer. From the magnetization (M)−temperature (T) curves (see the Supporting Information), their Curie temperatures (T_c) are calculated to be 208, 252, 257, and 275 K for $x = 0$, 0.3, 0.5, and 0.7, which increases with the doped Sr atom enhancement.[14] The hysteresis loops for all samples at 5 K (Figure 5) indicate that they have lower coercivity than the corresponding bulk materials. This originates from the surface spin disorder enhancment caused by the decreasing particle size,[15] and the coercivity would approach zero under a short thermal fluctuation (so-called super-paramagnetism) if the crystal size is small enough. On the other hand, the hysteresis loops become more and more asymmetric with the increase in Sr doping content, meaning exchange bias occurs. The enlarged magnetization curve of $La_{0.3}Sr_{0.7}MnO_3$ nanoparticles at 5 K (the inset of Figure 5) clearly illustrates the asymmetric hysteresis loop. For $x = 0$, 0.3, 0.5, and 0.7, the H_C values are 400, 225, 310, and 450 Oe, and the H_E values (the distance of loop shifts) are 0, 25, 40, and 120 Oe, respectively. Although the mechanism for the EB phenomenon of pure nanoparticle is elusive, it is believed to be related to the surface layer of the particles, because the change in the atomic coordination forms a layer of disordered spins and the particles behave as two magnetic systems.[16] The LSMO nanoparticles have an organic shell, which leads to their surface layer being different from the interior and induces the spin disorder.[17]

In summary, a series of crystalline LSMO nanoparticles without agglomeration in water have been prepared through the molten salt method following reaction in 2-pyrrolidone. Because many oxides nanoparticles could be synthesized by the molten salts method,[18] the process described in this article should be a general route to the aggregate-free oxide nanoparticles dispersed in water. The EB phenomenon found in LSMO nanoparticles offers rich insight inti their properties and may be useful in controlling their magnetization in devices where the EB might help to overcome the superparamagnetic limit.[19]

Acknowledgment. This work was supported by the Program for New Century Excellent Talents in University, P. R. China.

Supporting Information Available: Details of characterization, including the photographs of the aqueous suspension of LSMO nanoparticles, EDX spectrum, the TG curve, IR spectrum, $T-M$ curve, and experiments. This material is available free of charge via the Internet at http://pubs.acs.org.

CM0622349

(14) (a) Dabrowski, B.; Xiong, X.; Bukowski, Z.; Dybzinski, R.; Klamut, P. W.; Siewenie, J. E.; Chmaissem, O.; Shaffer, J.; Kimball, C. W.; Jorgensen, J. D.; Short, S. *Phys. Rev. B* **1999**, *60*, 7006. (b) Gupta, A.; McGuire, T. R.; Duncombe, P. R.; Rupp, M.; Sun, J. Z.; Gallagher, W. J.; Xiao, G. *Appl. Phys. Lett.* **1995**, *67*, 3494.

(15) Labaye, Y.; Crisan, O.; Berger, L.; Greneche, J. M.; Coey, J. M. O. *J. Appl. Phys.* **2002**, *91*, 8715.

(16) Nogués, J.; Schuller, I. K. *J. Magn. Magn. Mater.* **1999**, *192*, 203.

(17) Kodama, R. H.; Berkowitz, A. E.; McNiff, E. J.; Foner, S., Jr. *Phys. Rev. Lett.* **1996**, *77*, 394.

(18) (a) Mao, Y.; Banerjee, S.; Wong, S. S. *J. Am. Chem. Soc.* **2003**, *125*, 15718. (b) Mao, Y.; Wong, S. S. *Adv. Mater.* **2005**, *17*, 2194. (c) Geselbracht, M. J.; Noailles, L. D.; Ngo, L. T.; Pikul, J. H.; Walton, R. I.; Cowell, E. S.; Millange, F.; O'Hare, D. *Chem. Mater.* **2004**, *16*, 1153.

(19) (a) Skumryev, V.; Stoyanov, S.; Zhang, Y.; Hadjipanayis, G.; Givord, D.; Nogués, J. *Nature* **2003**, *423*, 850. (b) Jiang, Y.; Nozaki, T.; Abe, S.; Ochiai, T.; Hirohata, A.; Tezuka, N.; Inomata, K. *Nat. Mater.* **2004**, *3*, 361.